Cooperatively enhanced reactivity and "stabilitaxis" of dissociating oligomeric proteins

Jaime Agudo-Canalejo[a,b,c], Pierre Illien[d], and Ramin Golestanian[a,b,1]

[a]Department of Living Matter Physics, Max Planck Institute for Dynamics and Self-Organization, D-37077 Göttingen, Germany; [b]Rudolf Peierls Centre for Theoretical Physics, University of Oxford, Oxford OX1 3PU, United Kingdom; [c]Department of Chemistry, The Pennsylvania State University, University Park, PA 16802; and [d]Sorbonne Université, CNRS, Laboratoire Physicochimie des Electrolytes et Nanosystèmes Interfaciaux (PHENIX), UMR CNRS 8234, 75005 Paris, France

Edited by David A. Weitz, Harvard University, Cambridge, MA, and approved April 14, 2020 (received for review November 8, 2019)

Many functional units in biology, such as enzymes or molecular motors, are composed of several subunits that can reversibly assemble and disassemble. This includes oligomeric proteins composed of several smaller monomers, as well as protein complexes assembled from a few proteins. By studying the generic spatial transport properties of such proteins, we investigate here whether their ability to reversibly associate and dissociate may confer on them a functional advantage with respect to nondissociating proteins. In uniform environments with position-independent association–dissociation, we find that enhanced diffusion in the monomeric state coupled to reassociation into the functional oligomeric form leads to enhanced reactivity with localized targets. In nonuniform environments with position-dependent association–dissociation, caused by, for example, spatial gradients of an inhibiting chemical, we find that dissociating proteins generically tend to accumulate in regions where they are most stable, a process that we term "stabilitaxis."

protein complexes | intracellular transport | first passage | reactivity | self-organization

It has become increasingly clear in recent years that, in order to fully understand intracellular reaction pathways, it is not sufficient to know reaction rates and equilibrium constants: Understanding the transport properties of the biomolecules involved is also crucial (1). For example, it is now known that many enzymes undergo enhanced diffusion as well as chemotaxis in the presence of their chemical substrates (2–9). In turn, chemotaxis in response to chemicals that are being produced or consumed may lead to spontaneous self-organization of catalytic particles into chemically active clusters (10–12). Other works have shown the importance of segregation of different biomolecular components into phase-separated fluid compartments within the cell (13, 14), or how differences in diffusion coefficients between membrane-bound and cytosolic molecules are crucial for pattern formation and polarization in cells (15–20).

One particularly ubiquitous feature of functional units in biology, be it proteins, enzymes, or molecular machines, is that they are oligomeric, that is, complexes composed of several subunits that can reversibly associate and dissociate (21–31). These proteins are typically fully functional only in their oligomeric state. One may thus wonder why oligomers are so prevalent, rather than highly stable proteins and protein complexes with irreversibly bound components. We note that, physically, reversibility implies that the associated binding energies and energy barriers are of the order of the thermal energy $k_B T$ (where k_B is the Boltzmann constant and T is temperature). Could there be, perhaps, a functional advantage to proteins being able to disassemble and reassemble?

Inspired by this puzzle, we investigate here the transport properties of dissociating proteins (Fig. 1). One important question is how association–dissociation might affect the reactivity of a protein that needs to reach and react with a given target. Such problems, in which a protein diffuses until it finds a certain target, are typically known as "first passage" problems, and have been subject of many studies in recent years. The effects of different spatial geometries and heterogeneous media (32–36), anomalous diffusion (37, 38), or intermittently switching transport kinetics of the protein (39–42) on first passage times have all been explored, to a certain extent. A common feature of all these studies, however, is that they deal with systems of noninteracting particles, in which each particle behaves independently from the others: The first passage time is thus related only to the transport properties of a single particle, and is independent of particle concentrations.

This is not the case for dissociating proteins; see Fig. 1*C*. Indeed, whereas dissociation does occur independently for each protein, reassociation requires that two protein subunits find each other, and is thus dependent on the overall protein concentration in the system. The first passage time, therefore, becomes a collective property of the system. In fact, we find that association–dissociation can lead to an enhancement in reactivity with respect to a stable nondissociating protein, but this occurs cooperatively, only for protein concentrations above a critical value. Enhanced reactivity due to association–dissociation is thus a markedly different phenomenon than that obtained in switching diffusion models (41, 42), which represent, for example, a protein undergoing conformational changes.

A second important question with regards to the transport properties of oligomeric proteins is how they respond to heterogeneous environments; see Fig. 1*D*. We demonstrate here that dissociating proteins tend to spontaneously accumulate in regions in which they are most stable, via a generic mechanism which we term "stabilitaxis." This behavior may be exploited in order to trigger nonuniform patterns of protein in response

Significance

To gain insight into cellular metabolism, it is important to understand how proteins travel and self-organize within the cell. A characteristic feature of many important proteins is that they are oligomeric complexes, that is, they are composed of a few smaller subunits that can reversibly associate and dissociate. Here, we study the impact of dissociation on protein transport and self-organization. We find that dissociation can help proteins find and react with a target more rapidly, and that dissociating proteins spontaneously accumulate in regions in which they are most stable.

Author contributions: J.A.-C., P.I., and R.G. designed research; J.A.-C. performed research; J.A.-C., P.I., and R.G. analyzed data; J.A.-C. and R.G. wrote the paper; and J.A.-C., P.I., and R.G. contributed to the discussion of the results and commented on the manuscript.

The authors declare no competing interest.

This article is a PNAS Direct Submission.

[1]To whom correspondence may be addressed. Email: ramin.golestanian@ds.mpg.de.

This article contains supporting information online at https://www.pnas.org/lookup/suppl/doi:10.1073/pnas.1919635117/-/DCSupplemental.

First published May 15, 2020.

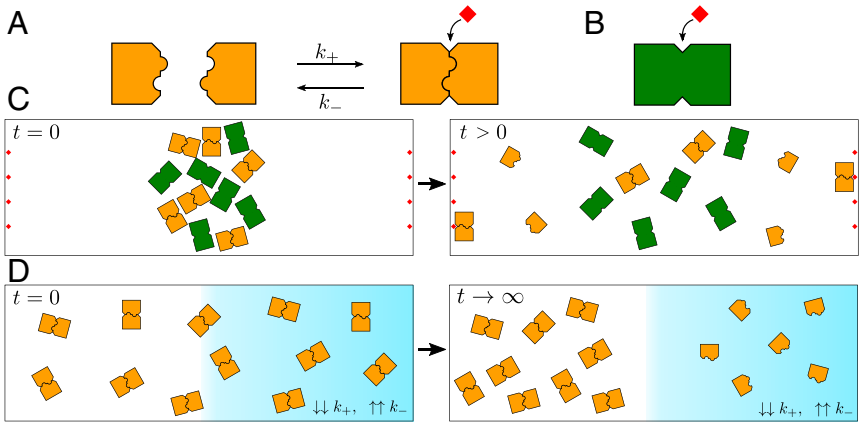

Fig. 1. (*A*) Minimal model of an oligomeric protein. The monomers of a homodimeric protein can associate and dissociate with rates k_+ and k_-, which may be dependent on environmental conditions (concentration of salt or a chemical inhibitor, pH, illumination, etc.). The protein is functional (in this case, able to bind and react with the red ligand) only in its dimer form. (*B*) A nondissociating but otherwise identical protein. (*C*) Faster diffusion of the monomers coupled to reassociation into dimers helps a dissociating protein reach a reactive target in less time than its nondissociating counterpart. (*D*) In the presence of externally imposed spatial gradients of the dissociation rates, dissociating proteins undergo stabilitaxis; that is, they tend to accumulate in regions where the oligomeric form is most stable.

to gradients of any stimuli that affects protein stability, be it concentration of a chemical inhibitor, salt, pH, or light.

The paper is organized as follows. In *Results*, we first describe the basic model for a dissociating homodimer protein, and predict enhanced diffusion and stabilitaxis arising from dissociation. We then show how enhanced diffusion coupled to reassociation leads to enhanced reactivity with localized targets through a cooperative mechanism, and demonstrate how stabilitaxis leads to nonuniform steady-state patterns of protein in the presence of dissociation gradients. Finally, in *Discussion*, we embed our results within the context of biology and materials engineering.

Results

Enhanced Diffusion and Dissociation-Induced Drift Velocity. We consider the simplest model for the reversible association and dissociation of two identical monomers to form a homodimeric protein; see Fig. 1*A*. The concentrations of monomer and of dimer, respectively, ρ_1 and ρ_2, are governed by the coupled time evolution equations

$$\begin{aligned}\partial_t\rho_1 &= D_1\nabla^2\rho_1 - 2k_+\rho_1^2 + 2k_-\rho_2,\\ \partial_t\rho_2 &= D_2\nabla^2\rho_2 + k_+\rho_1^2 - k_-\rho_2,\end{aligned} \qquad [1]$$

where both the association and dissociation rates k_+ and k_- can depend arbitrarily on the environmental conditions (concentration of salt or a chemical inhibitor, pH, illumination, etc.), which, in turn, may be space dependent. The monomer diffuses with coefficient D_1, and the dimer diffuses with coefficient D_2. Note that, in general, the bulkier dimer will diffuse more slowly than the monomer, so that $D_2 < D_1$. In fact, we have shown in previous work that, for two subunits that are linked into a dimer, the diffusion coefficient of the dimer goes as $D_2 = D_1/2 - \delta D_{\rm fluc}$, where $\delta D_{\rm fluc} > 0$ corresponds to a fluctuation-induced hydrodynamic correction (43–45). We therefore generically expect the even stronger condition $D_2 < D_1/2$.

Direct analytical solution of the coupled nonlinear evolution equations in Eq. **1** is hard. However, further progress can be achieved if we focus on the total protein concentration $\rho_{\rm tot} \equiv \rho_1/2 + \rho_2$, defined as the equivalent amount of dimeric protein, where the factor $1/2$ reflects the fact that two monomers are needed to generate a dimer. Summing both equations, we can write an evolution equation for the total protein concentration given by

$$\partial_t\rho_{\rm tot} = \frac{D_1}{2}\nabla^2\rho_1 + D_2\nabla^2\rho_2. \qquad [2]$$

For sufficiently weak protein gradients, the typical timescale for diffusion is much slower than the association–dissociation timescale, and we can make a local equilibrium approximation $k_+\rho_1^2 \approx k_-\rho_2$, implying that ρ_1 and ρ_2 quickly equilibrate at every point in space. Under this approximation, the local monomer and dimer concentrations are related to the local total protein concentration by

$$\rho_1 \approx \frac{K_{\rm d}}{4}\left(\sqrt{1+16\frac{\rho_{\rm tot}}{K_{\rm d}}}-1\right), \quad \text{and} \quad \rho_2 \approx \frac{\rho_1^2}{K_{\rm d}}, \qquad [3]$$

where we have defined the dissociation constant $K_{\rm d} \equiv k_-/k_+$, which carries the environment dependence (or position dependence) of the association and dissociation rates.

Inserting the values resulting from the local equilibrium approximation into Eq. **2**, we finally obtain an explicit evolution equation for the total protein concentration,

$$\partial_t\rho_{\rm tot} = \nabla\cdot(D_{\rm eff}\nabla\rho_{\rm tot} - \rho_{\rm tot}\boldsymbol{V}_{\rm dis}), \qquad [4]$$

with the effective diffusion coefficient

$$D_{\rm eff} \equiv D_2 + \frac{D_1 - D_2}{\sqrt{1+16\rho_{\rm tot}/K_{\rm d}}}, \qquad [5]$$

and the dissociation-induced drift velocity

$$\boldsymbol{V}_{\rm dis} \equiv -\frac{D_1 - D_2}{8}\left(\frac{1+8\rho_{\rm tot}/K_{\rm d}}{\sqrt{1+16\rho_{\rm tot}/K_{\rm d}}}-1\right)\frac{\nabla K_{\rm d}}{\rho_{\rm tot}}. \qquad [6]$$

Because the dimer diffuses more slowly than the monomer, with $D_2 < D_1$, the effective diffusion coefficient is always larger than the dimer diffusion coefficient, $D_{\rm eff} > D_2$; that is, dissociation leads to enhanced diffusion. The effective diffusion coefficient decreases monotonically with increasing protein concentration, from $D_{\rm eff} = D_1$ at low protein concentration ($\rho_{\rm tot} \ll K_{\rm d}$, in which case all proteins are in the form of monomers) to $D_{\rm eff} = D_2$ at high protein concentrations ($\rho_{\rm tot} \gg K_{\rm d}$, in which case all proteins are in the form of dimers). Equivalently, the effective diffusion coefficient increases monotonically with increasing $K_{\rm d}$, from $D_{\rm eff} = D_2$ to $D_{\rm eff} = D_1$.

Noting that the coefficient multiplying $\nabla K_{\rm d}$ in Eq. **6** is always negative, we see that the dissociation-induced velocity

$\boldsymbol{V}_{\rm dis}$ always points in the direction of decreasing $K_{\rm d}$, which is toward regions where the dimer is more stable. We term this behavior stabilitaxis. Moreover, we note that the magnitude of the velocity depends nonmonotonically on the protein concentration, tending to zero for low ($\rho_{\rm tot} \ll K_{\rm d}$) and high ($\rho_{\rm tot} \gg K_{\rm d}$) protein concentrations, and reaching a maximum value at $\rho_{\rm tot} \simeq 0.3 K_{\rm d}$.

The approach that we just followed, based on using the local equilibrium approximation in order to obtain a closed evolution equation for the total protein concentration in a reaction–diffusion system with mass conservation, has been developed in great detail in the context of pattern formation by systems that exhibit a Turing instability (16–18). In these studies, the reaction rates are typically position independent [or at most, varying step-wise (18)], but the system itself can become laterally unstable. In the problem that we consider here, on the other hand, the association–dissociation rates may have an arbitrary space dependence, but the system would otherwise be laterally stable. The local equilibrium approximation was also used in the latter context in ref. 5, which studied enzyme chemotaxis in response to arbitrary substrate gradients.

Cooperatively Enhanced Reactivity. We have shown that the effective diffusion of the total amount (in both monomeric and dimeric form) of a dissociating protein is faster than that of a nondissociating protein; that is, we always have $D_{\rm eff} > D_2$. This conclusion was to be expected, given that the smaller monomers will diffuse faster than the bulkier dimers. A less obvious question, and one more relevant to biology as well as technological applications, is whether association–dissociation can help a protein reach and react with a distant reactive target more rapidly. Note that, while dissociation helps in enhancing diffusion, it also hinders the reaction by rendering the protein nonfunctional, which suggests a nontrivial competition between these two effects.

To this end, we have investigated the first passage time of dimers placed at the center of a one-dimensional (1D) domain of length L, with absorbing boundary conditions for the dimers [$\rho_2(x=0) = \rho_2(x=L) = 0$] and no-flux boundary conditions [$\rho_1'(x=0) = \rho_1'(x=L) = 0$] for the monomers. This represents a system in which a target located at the boundaries reacts instantaneously with dimers (diffusion-limited reaction) but is insensitive to monomers. The results for the dissociating case, obtained from numerical solution of the coupled partial differential equations in Eq. **1** with position-independent k_+ and k_-, are compared with those for the diffusion of a nondissociating protein, governed simply by $\partial_t \rho_2^{\rm nd} = D_2 \nabla^2 \rho_2^{\rm nd}$ (see *Methods*).

Because dimers are absorbed at the boundaries, the total protein number $N(t) = N_1(t)/2 + N_2(t)$ within the box decreases with time. Here, N_1 and N_2 are the monomer and dimer numbers, with $N_i = \int_0^L \rho_i {\rm d}x$. We can then define a time-dependent reaction rate as $R(t) = -[1/N(t=0)]{\rm d}N/{\rm d}t$. The reaction rate defined in this way verifies the normalization condition $\int_0^\infty R(t){\rm d}t = 1$, and serves as a mean-field generalization of the first passage time probability distribution to a system with many interacting particles, which will coincide with the results of a stochastic approach in the limit of a large number of particles.

We find that, in a system of associating and dissociating particles, first passage is indeed a collective property of the system (Fig. 2). In particular, the reaction rate curve $R(t)$ depends on the total initial protein number, as given by the number $N_2(t=0) \equiv \rho_{2,0} L$ of dimers initially placed at the center of the box. The $R(t)$ curves for several values of $\rho_{2,0}$ are shown in Fig. 2*A* and compared with that of a nondissociating protein (black dotted line). At low concentrations, the dissociating protein is mostly in monomer form, and reacts more slowly than a nondissociating protein (red line). At intermediate values of protein concentration, however, a positive interplay between faster diffusion in the monomer state, coupled to sufficiently frequent reassociation into the reactive dimer state, leads to enhanced reactivity with respect to the nondissociating protein (yellow line). As the protein concentration is further increased, the proteins spend most of the time in the dimer state and react with a rate very similar to a nondissociating protein (green line).

Enhanced reactivity thus arises as a cooperative effect from the interaction of a sufficiently large number of proteins. This is clearly seen in Fig. 2*B*, which shows both the median first passage time t_{50} and the peak reaction rate $R_{\rm max}$, relative to those of a nondissociating protein $t_{50}^{\rm nd}$ and $R_{\rm max}^{\rm nd}$, as a function of protein concentration. The median first passage time obtained from $R(t)$ is a mean-field quantity representing the time after which 50% of the initial proteins have reacted with the target, which, for a many-particle system such as the one under consideration, is a more intuitive measure of reaction speed than the mean first passage time.

Moreover, we find that reactivity is enhanced when the dynamics of association–dissociation is sufficiently fast as compared to the diffusion timescale; see Fig. 2*C*. For very slow dynamics, with $k_- L^2/D_1 \ll 1$, the protein does not have time to dissociate before reaching the target, and thus behaves effectively as a nondissociating protein. At intermediate values, dissociation is counterproductive, as the protein has sufficient time to dissociate before reaching the target, but still takes a long time to reassociate in order to react. Finally, when the dynamics becomes sufficiently fast, dissociation is always favorable, as it enhances diffusion (Eq. **5**), while reassociation is fast enough to not hinder the reaction.

The combined effect of protein concentration and association–dissociation dynamics on the median first passage time is summarized in Fig. 2*D*, for the particular case $D_2 = 0.5 D_1$. Cooperatively enhanced reactivity is found at an intermediate range of protein concentrations and for sufficiently fast association–dissociation dynamics. The optimal value of concentration that minimizes the median first passage time decreases with increasing k_- (yellow line). Within the range of values explored, the median first passage time can be up to 40% smaller for a dissociating protein than for a nondissociating protein, and will decrease even further for larger values of $k_- L^2/D_1$. Note that our results remain qualitatively similar if a measure of reaction speed other than the median first passage time is used. As an example, we also show the line $t_{99} = t_{99}^{\rm nd}$ (dotted line), representing the values above which the time it takes for 99% of the proteins to react is shorter for a dissociating protein than for a nondissociating one.

The enhancement in reactivity (reduction in median first passage time) that can be achieved due to dissociation increases as the ratio D_2/D_1 is decreased; see *SI Appendix*, Fig. S1 for the case $D_2/D_1 = 0.3$. In fact, we expect that the minimal median first passage time that can be achieved is $t_{50} = (D_2/D_1) t_{50}^{\rm nd}$, which will occur in the limit in which the protein concentration is very low, $\rho_{2,0} \ll K_{\rm d}$. In this regime, the protein is mostly in monomer form. However, if the association and dissociation rates are very fast, namely, $k_- L^2/D_1 \gg 1$, reassociation can occur very rapidly near the target. Note that all of the results just described were obtained from numerical solution of the full evolution equations (Eq. **1**) at finite $k_- L^2/D_1$. In order to examine the limit of very fast association–dissociation, we can, instead, consider the first passage time problem using the local equilibrium approximation in Eq. **4**, which, in fact, corresponds to the limit $k_- L^2/D_1 \to \infty$. We have solved this equation numerically, for the case $D_2 = 0.5 D_1$, to obtain the median first passage time as a function of total protein concentration, and, indeed, we find that the first passage time goes from that expected of a monomer

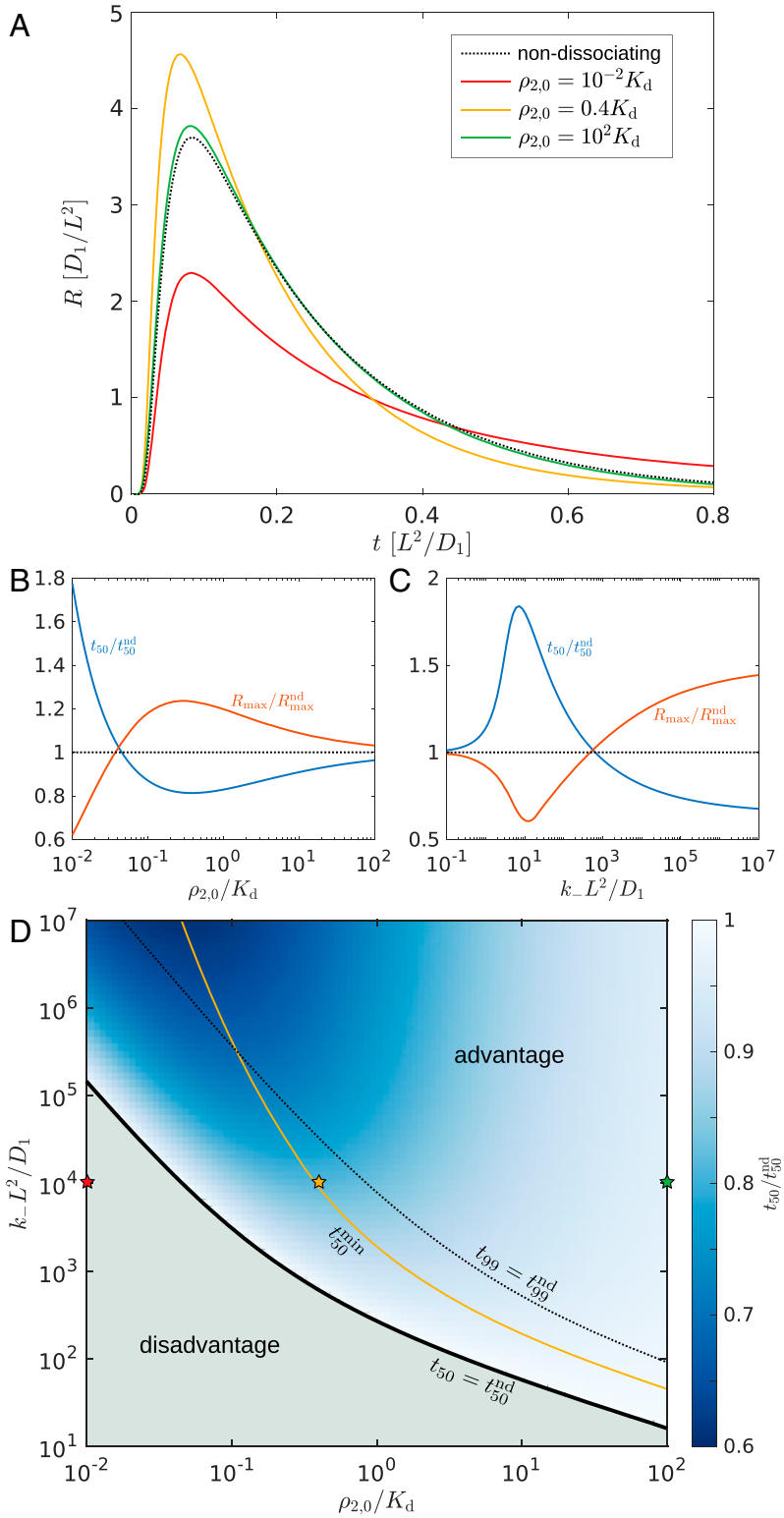

Fig. 2. (*A*) Reaction rate as a function of time for a dissociating protein at three different concentrations, as well as that of a nondissociating protein. (*B* and *C*) Median first passage time t_{50} (time at which half of all proteins have reacted) and maximal reaction rate R_{max} relative to those of a nondissociating protein t_{50}^{nd} and $R_{\mathrm{max}}^{\mathrm{nd}}$ (*B*) as a function of protein concentration and (*C*) as a function of $k_- L^2/D_1$ which compares the rate of association–dissociation to the diffusion rate. (*D*) The $t_{50}/t_{50}^{\mathrm{nd}}$ as a function of both protein concentration and association–dissociation rate. The "disadvantage" region corresponds to $t_{50}/t_{50}^{\mathrm{nd}} > 1$; the red, yellow, and green stars refer to the reaction rate curves in *A*; the line labeled t_{50}^{min} indicates the concentrations that minimize t_{50} for a given k_-; and the line $t_{99} = t_{99}^{\mathrm{nd}}$ denotes the values above which 99% of the proteins react faster in the dissociating case. In all cases, we set $D_2 = 0.5 D_1$; in *A* and *B*, $k_- L^2/D_1 = 10^4$; and, in *C*, $\rho_{2,0} = 0.4 K_\mathrm{d}$.

($t_{50} = 0.5 t_{50}^{\mathrm{nd}}$) at very low concentration to that expected of a dimer ($t_{50} = t_{50}^{\mathrm{nd}}$) at very high concentration (*SI Appendix*, Fig. S2). Note that the limit $k_- L^2/D_1 \to \infty$ corresponding to the local equilibrium approximation shows qualitatively different behavior than that seen at finite $k_- L^2/D_1$, because, in this limit, there is no optimal concentration for which the median first passage time is minimal; instead, the first passage time increases monotonically with increasing concentration. This implies that the optimal concentration tends to zero as $k_- L^2/D_1$ tends to infinity.

The results just described were obtained for the first passage time of dimers initially placed at the center of a 1D domain with reactive boundaries, but our results hold more generally. In particular, we find that dimensionality does not play a role, and dimers placed at the center of a two-dimensional (2D) circular domain or a three-dimensional (3D) spherical domain with reactive boundaries also show cooperatively enhanced reactivity, with nearly identical enhancements (*SI Appendix*, Fig. S3). Moreover, cooperatively enhanced reactivity is also robust to the choice of initial conditions for the monomer and dimer distributions. As a particularly relevant example, we have considered, as initial condition, a laterally uniform distribution of monomers and dimers at association–dissociation equilibrium ($\rho_2 = \rho_1^2/K_\mathrm{d}$), instead of a highly concentrated distribution of dimers at the center of the domain. This would correspond to a case in which the system is first allowed to relax to equilibrium in the absence of the boundary reaction, and then the boundary reaction is switched on. We find that there is also cooperatively enhanced reactivity for this choice of initial conditions, with very similar enhancements as above (*SI Appendix*, Fig. S4).

Stabilitaxis: Accumulation in Regions of Higher Stability. The existence of the dissociation-induced drift velocity (Eq. **6**) suggests that, in environments with position-dependent dissociation, dissociating proteins will tend to preferentially accumulate in the regions of higher stability after some time. Indeed, we can verify the existence of such stabilitaxis by calculating the steady-state concentrations for the monomer, dimer, and total amount of protein in a nonuniform environment. From Eq. **2**, we see that the total flux of protein is given by $\boldsymbol{J} = -\nabla(D_1\rho_1/2 + D_2\rho_2)$. Requiring that this flux be equal to zero, $\boldsymbol{J} = 0$, we find that, in a steady state with no influx or outflux of proteins into the system, the combination $D_1\rho_1/2 + D_2\rho_2$ must be a position-independent constant. Combining this condition with the results of the local equilibrium approximation in Eq. **3**, we finally find the steady-state profiles

$$\rho_{1,\infty} \approx \frac{K_\mathrm{d}}{4}\frac{D_1}{D_2}\left(-1+\sqrt{1+\frac{C}{K_\mathrm{d}}}\right),$$
$$\rho_{2,\infty} \approx \frac{\rho_{1,\infty}^2}{K_\mathrm{d}}, \text{ and } \rho_{\mathrm{tot},\infty} \approx \frac{\rho_{1,\infty}}{2} + \frac{\rho_{1,\infty}^2}{K_\mathrm{d}}, \qquad [7]$$

where C is a constant with units of concentration, which is used to satisfy the constraint on the total amount of protein. The same approach, based on combining the local equilibrium approximation with the condition of zero total protein flux at steady state, has been recently used to understand pattern formation in reaction–diffusion systems that display a lateral instability, including a novel geometric interpretation of the concepts of local equilibrium and zero total flux, both in the case of spatially uniform reaction rates (17) and in environments with a step-wise position dependence of the reaction rates (18).

To confirm the validity of our steady-state results, we have compared them to the long time limit of the numerical solution of the coupled partial differential equations (Eq. **1**), with no-flux boundary conditions $\rho_1'(x=0) = \rho_2'(x=0) = \rho_1'(x=L) = \rho_2'(x=L) = 0$ for all species, for two different examples of position-dependent association and dissociation rates k_+ and k_-, which naturally lead to a position-dependent $K_\mathrm{d} = k_-/k_+$ (Fig. 3). The steady-state profile given by Eq. **7** reproduces well the numerical results, although it deviates near the box boundaries. This can be understood by noting that the no-flux boundary conditions are not appropriately captured by the local equilibrium approximation, nor are regions with sharp changes in K_d and thus in the protein concentration. The width of the region over which deviations are significant is governed by the length scale $\sqrt{D_1/k_-}$, as can be understood from a first-order approximation valid for small deviations around the local equilibrium approximation (*SI Appendix*). Therefore, these deviations become progressively smaller, and the local equilibrium approximation becomes increasingly more accurate, with increasing $k_- L^2/D_1$ (*SI Appendix*, Fig. S5). As

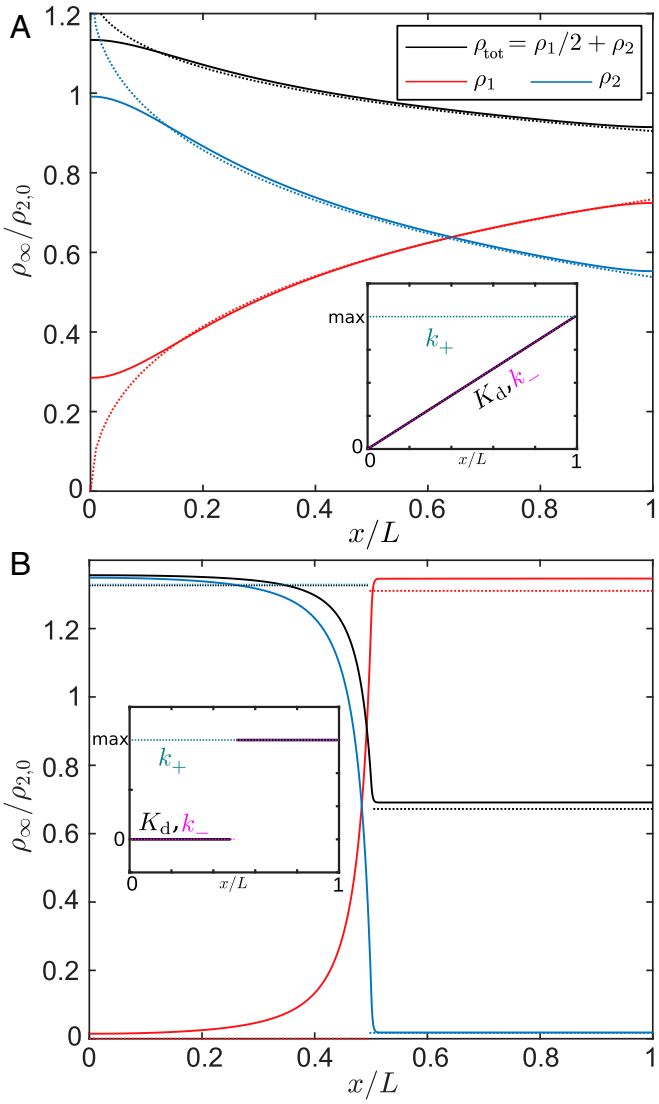

Fig. 3. Steady-state concentrations for a protein in the presence of a dissociation gradient. The numerical solution of Eq. **1** (solid lines) can be compared to the local equilibrium approximation in Eq. **7** (dotted lines). The protein undergoes stabilitaxis, accumulating in regions of higher stability. *Insets* show the corresponding dissociation gradients (arbitrary units): (*A*) linear gradient in k_- leading to linearly increasing K_d; and (*B*) discrete jump in k_- and thus K_d. In both cases, we have set $D_2 = 0.5 D_1$. In *A*, $k_-^{\mathrm{max}} L^2/D_1 = 10^2$ and $\rho_{2,0} = K_\mathrm{d}^{\mathrm{max}}$. In *B*, $k_-^{\mathrm{max}} L^2/D_1 = 10^5$ and $\rho_{2,0} = 10^{-2} K_\mathrm{d}^{\mathrm{max}}$.

predicted, the protein does preferentially accumulate in regions of higher stability (lower K_d), whether one considers the total protein amount including monomer and dimer forms (black lines), or just the dimer form (blue lines). These results are independent of the dimensionality of the system, and we obtain similar profiles, well captured by the local equilibrium approximation, for 2D and 3D circular and spherical domains (*SI Appendix*, Fig. S6). The fact that the steady-state profiles depend on the ratio of diffusion coefficients (see Eq. **7**) clearly demonstrates that stabilitaxis is a nonequilibrium phenomenon, which must be sustained by externally imposed gradients.

The dependence of stabilitaxis on the ratio of diffusion coefficients is most evident if we consider the limit of a space containing two connected regions; one with very weak dissociation $K_d \to 0$, for which we expect $\rho_{tot} \approx \rho_2$ and $\rho_1 \approx 0$, and the other with very strong dissociation $K_d \to \infty$, for which we expect $\rho_{tot} \approx \rho_1/2$ and $\rho_2 \approx 0$. Taking these limits in Eq. **7**, and solving for C, we obtain the relation

$$D_2 \rho_{tot,\infty}(K_d \to 0) \approx D_1 \rho_{tot,\infty}(K_d \to \infty), \qquad [8]$$

between the protein concentrations in both regions. For $D_2 = 0.5 D_1$, we thus expect twice as much protein in the region where it is stable as compared to the region where it is unstable. This prediction is confirmed by the numerical result in Fig. 3*B*.

In order for a protein gradient to be established via stabilitaxis, the underlying dissociation gradient should be sufficiently long lived. The typical timescale over which the steady-state distribution is reached is given by L^2/D_1, and thus the required minimal lifetime of the underlying gradient will strongly depend on the system size. Using $D_1 = 10\ \mu m^2/s$ as a typical protein diffusion coefficient in the cytoplasm, we find characteristic times of 0.1 s for a small cell with $L = 1\ \mu m$, 10 s for a cell with $L = 10\ \mu m$, or 1,000 s for a large cell with $L = 100\ \mu m$.

Discussion

We have predicted here a number of nontrivial features in the diffusion, reactivity, and gradient response of dissociating oligomeric proteins. Some of these features could be seen as conferring a functional advantage to dissociating proteins over nondissociating ones, which might explain why biological evolution has resulted in many important enzymes and proteins being multimeric.

Firstly, we have shown that it can be advantageous for a protein, enzyme, or molecular machine to dissociate into nonfunctional but smaller subunits that can diffuse faster, and later reassociate to perform their function at a distant location. This can lead to significantly faster reaction rates for dissociating proteins. We have shown that enhanced reactivity arises as a cooperative effect, which minimizes reaction time for an intermediate range of protein concentrations. Moreover, as can be seen from Fig. 2, dissociation becomes more and more advantageous with increasing values of the dimensionless quantity $k_- L^2/D_1$, which compares the rate of unbinding with the typical timescale of diffusion across the system. Crucially, this quantity scales with the square of the system size, and therefore can vary over many orders of magnitude for different systems. Experimental measurements of protein complex dissociation kinetics are not widely available, but some relevant examples can be found, such as $k_- \approx 20\ s^{-1}$ for the CheY–CheA complex involved in the sensory response pathway of *Escherichia coli* (46), or $k_- \approx 2\ s^{-1}$ for the p53–Mdm2 complex involved in DNA repair (47) as well as for the WASp–Cdc42 complex involved in the remodeling of actin filaments (48). Using a moderate choice of $k_- = 1\ s^{-1}$ for the dissociation rate (49–51), and $D_1 = 10\ \mu m^2/s$ for the diffusion coefficient of a protein in the cytoplasm, we find values of $k_- L^2/D_1$ ranging from 10^{-1} for a small cell with $L = 1\ \mu m$, to 10^3 for a large cell with $L = 100\ \mu m$, all of the way up to 10^7 for diffusion along a neuronal axon or a microfluidic device with $L = 1$ cm. For membrane-bound proteins, the diffusion coefficient is greatly reduced, and thus the corresponding values of $k_- L^2/D_1$ will be significantly enhanced, and the advantages due to dissociation will be greater. For any given protein, the advantages due to dissociation will be largest when the target to be reached is distant. The typical reactivity enhancements that can be achieved are of the order of D_1/D_2, and thus, for a dissociating dimer, are of the order of 10 to 50% (Fig. 2).

Secondly, we have shown that dissociation provides a mechanism for proteins to sense and respond to their environment, by undergoing stabilitaxis or motion toward regions in which their oligomeric form is most stable. Stabilitaxis represents a mechanism by which nonuniform patterns in the concentration of a biomolecule can be triggered. For example, polarization in the concentration of a dissociating protein within a cell can be triggered by localized production of a chemical that enhances or inhibits the association or dissociation of the protein subunits. The precise form of the resulting protein distribution can be predicted from Eq. **7**, but, in general, the typical difference in protein concentration between the regions of low and high dissociation will be proportional to D_1/D_2; see Eq. **8**. It remains to be seen whether stabilitaxis is exploited by the cell in the intracellular organization of oligomeric proteins.

Although we have focused here, for simplicity, on the case of a homodimeric protein, we expect that our general predictions of enhanced reactivity and stabilitaxis will hold equally for more complex cases of heteromultimeric proteins (i.e., composed of more than two subunits, that may also be different from each other). As an example of a more complex protein, we have considered a homohexamer, composed of six identical subunits, and found qualitatively similar results for both enhanced reactivity and stabilitaxis (*SI Appendix*, Fig. S7). Interestingly, our numerical results show that the prediction in Eq. **8** for stabilitaxis still holds if we replace the dimer diffusion coefficient by the hexamer diffusion coefficient. Because the ratio of monomer and hexamer diffusion coefficients is much larger (on the order of six), the protein accumulation due to stabilitaxis is enhanced significantly. We expect that the maximum achievable enhancement in reactivity (for sufficiently fast association–dissociation rate) will also be larger for a multimeric protein with a large difference in diffusion coefficient between the monomeric and multimeric forms.

Beyond the biological implications, our predictions of enhanced reactivity may be useful in the context of chemical engineering, for example, in the design of synthetic catalytic microreactors. Moreover, our results may also be tested and applied in purely synthetic systems, for example, using patchy colloids coated with ligands, that can bind to each other to form colloidal molecules. In the context of engineering of active or responsive materials, one particularly interesting application would be to use colloids coated with light-induced linkers (52) that bind to each other only when illuminated. Such a material would flow and become denser in illuminated regions on demand.

Materials and Methods

Numerical Solution of Evolution Equations. The coupled evolution equations, Eq. **1**, are numerically solved using MATLAB's pdepe solver for systems of parabolic partial differential equations (53). The size of the system is given by L, which, in 1D calculations, corresponds to the length of the domain, and, in 2D and 3D calculations, corresponds to the diameter of the circular or spherical domain. We can then define the dimensionless time as $\tau \equiv tD_1/L^2$, position as $\tilde{x} \equiv x/L$ in 1D calculations or as the radial coordinate $\tilde{r} \equiv r/L$ in 2D and 3D calculations, and concentrations as $\tilde{\rho} \equiv (k_+/k_-)\rho = \rho/K_d$. The system is then governed by two dimensionless parameters only, namely,

the ratio of association–diffusion timescales $\tilde{k}_- \equiv k_- L^2/D_1$, and the ratio of dimer-to-monomer diffusion coefficients $\tilde{D}_2 \equiv D_2/D_1$, as well as our choice of initial conditions. In cases with position-dependent k_-, we use the maximum value $k_-^{\max}$ for the nondimensionalization. For the initial conditions, we use (except for *SI Appendix*, Fig. S4) a Gaussian profile located at the center of the box for the concentration of the dimer, with standard deviation $\sigma = 0.01L$, and normalized so that the total amount of dimer in the box is $\rho_{2,0}L$; the initial concentration of the monomers is set to zero. We use 1,000 points in the space discretization. The system is evolved in time until 99% of the proteins have been consumed (when calculating the reaction rate), or until a steady state is reached (when exploring stabilitaxis).

Data Availability. All data are available in the paper and *SI Appendix*.

ACKNOWLEDGMENTS. We thank Jean-François Rupprecht for comments on an early version of the manuscript. J.A-C. and R.G. acknowledge funding from the NSF under Materials Research Science and Engineering Centers Grant DMR-1420620.

1. T. L. Hill, *Free Energy Transduction and Biochemical Cycle Kinetics* (Springer, New York, NY, 1989).
2. J. Agudo-Canalejo, T. Adeleke-Larodo, P. Illien, R. Golestanian, Enhanced diffusion and chemotaxis at the nanoscale. *Acc. Chem. Res.* **51**, 2365–2372 (2018).
3. A. Y. Jee, S. Dutta, Y. K. Cho, T. Tlusty, S. Granick, Enzyme leaps fuel antichemotaxis. *Proc. Natl. Acad. Sci. U.S.A.* **115**, 14–18 (2018).
4. K. K. Dey *et al.*, Chemotactic separation of enzymes. *ACS Nano* **8**, 11941–11949 (2014).
5. J. Agudo-Canalejo, P. Illien, R. Golestanian, Phoresis and enhanced diffusion compete in enzyme chemotaxis. *Nano Lett.* **18**, 2711–2717 (2018).
6. C. Riedel *et al.*, The heat released during catalytic turnover enhances the diffusion of an enzyme. *Nature* **517**, 227–230 (2015).
7. P. Illien *et al.*, Exothermicity is not a necessary condition for enhanced diffusion of enzymes. *Nano Lett.* **17**, 4415–4420 (2017).
8. A. Y. Jee, Y. K. Cho, S. Granick, T. Tlusty, Catalytic enzymes are active matter. *Proc. Nat. Acad. Sci. U.S.A.* **115**, E10812–E10821 (2018).
9. M. Xu, L. Valdez, A. Sen, J. L. Ross, Direct single molecule imaging of enhanced enzyme diffusion. *Phys. Rev. Lett.* **123**, 128101 (2019).
10. J. Agudo-Canalejo, R. Golestanian, Active phase separation in mixtures of chemically interacting particles. *Phys. Rev. Lett.* **123**, 018101 (2019).
11. F. Wu, L. N. Pelster, S. D. Minteer, Krebs cycle metabolon formation: Metabolite concentration gradient enhanced compartmentation of sequential enzymes. *Chem. Commun.* **51**, 1244–1247 (2015).
12. X. Zhao *et al.*, Substrate-driven chemotactic assembly in an enzyme cascade. *Nat. Chem.* **10**, 311–317 (2018).
13. S. Boeynaems *et al.*, Protein phase separation: A new phase in cell biology. *Trends Cell Biol.* **28**, 420–435 (2018).
14. B. S. Schuster *et al.*, Controllable protein phase separation and modular recruitment to form responsive membraneless organelles. *Nat. Commun.* **9**, 1–12 (2018).
15. J. Halatek, F. Brauns, E. Frey, Self-organization principles of intracellular pattern formation. *Phil. Trans. Biol. Sci.* **373**, 20170107 (2018).
16. J. Halatek, E. Frey, Rethinking pattern formation in reaction-diffusion systems. *Nat. Phys.* **14**, 507–514 (2018).
17. F. Brauns, J. Halatek, E. Frey, Phase-space geometry of reaction-diffusion dynamics. arXiv:1812.08684 (20 December 2018).
18. M. C. Wigbers, F. Brauns, T. Hermann, E. Frey, Pattern localization to a domain edge. *Phys. Rev.* **101**, 022414 (2020).
19. B. Ramm *et al.*, The MinDE system is a generic spatial cue for membrane protein distribution in vitro. *Nat. Commun.* **9**, 3942 (2018).
20. P. Gross *et al.*, Guiding self-organized pattern formation in cell polarity establishment. *Nat. Phys.* **15**, 293–300 (2019).
21. T. W. Traut, Dissociation of enzyme oligomers: A mechanism for allosteric regulation. *Crit. Rev. Biochem. Mol. Biol.* **29**, 125–163 (1994).
22. G. D'Alessio, The evolutionary transition from monomeric to oligomeric proteins: Tools, the environment, hypotheses. *Prog. Biophys. Mol. Biol.* **72**, 271–298 (1999).
23. M. H. Ali, B. Imperiali, Protein oligomerization: How and why. *Bioorg. Med. Chem.* **13**, 5013–5020 (2005).
24. I. André, C. E. Strauss, D. B. Kaplan, P. Bradley, D. Baker, Emergence of symmetry in homooligomeric biological assemblies. *Proc. Nat. Acad. Sci. U.S.A.* **105**, 16148–16152 (2008).
25. E. D. Levy, E. B. Erba, C. V. Robinson, S. A. Teichmann, Assembly reflects evolution of protein complexes. *Nature* **453**, 1262–1265 (2008).
26. A. S. Coquel *et al.*, Localization of protein aggregation in *Escherichia coli* is governed by diffusion and nucleoid macromolecular crowding effect. *PLoS Comput. Biol.* **9**, e1003038 (2013).
27. S. E. Ahnert, J. A. Marsh, H. Hernández, C. V. Robinson, S. A. Teichmann, Principles of assembly reveal a periodic table of protein complexes. *Science* **350**, aaa2245 (2015).
28. H. Garcia-Seisdedos, C. Empereur-Mot, N. Elad, E. D. Levy, Proteins evolve on the edge of supramolecular self-assembly. *Nature* **548**, 244–247 (2017).
29. J. P. Günther, M. Börsch, P. Fischer, Diffusion measurements of swimming enzymes with fluorescence correlation spectroscopy. *Acc. Chem. Res.* **51**, 1911–1920 (2018).
30. A. Y. Jee, K. Chen, T. Tlusty, J. Zhao, S. Granick, Enhanced diffusion and oligomeric enzyme dissociation. *J. Am. Chem. Soc.* **141**, 20062–20068 (2019).
31. M. Hidalgo-Soria, E. Barkai, The Hitchhiker model for Laplace diffusion processes in the cell environment. arXiv:1909.07189 (16 September 2019).
32. S. Condamin, O. Bénichou, V. Tejedor, R. Voituriez, J. Klafter, First-passage times in complex scale-invariant media. *Nature* **450**, 77–80 (2007).
33. O. Bénichou, C. Chevalier, J. Klafter, B. Meyer, R. Voituriez, Geometry-controlled kinetics. *Nat. Chem.* **2**, 472–477 (2010).
34. T. G. Mattos, C. Mejía-Monasterio, R. Metzler, G. Oshanin, First passages in bounded domains: When is the mean first passage time meaningful? *Phys. Rev.* **86**, 031143 (2012).
35. T. Guérin, N. Levernier, O. Bénichou, R. Voituriez, Mean first-passage times of non-Markovian random walkers in confinement. *Nature* **534**, 356–359 (2016).
36. A. Godec, R. Metzler, First passage time distribution in heterogeneity controlled kinetics: Going beyond the mean first passage time. *Sci. Rep.* **6**, 20349 (2016).
37. M. Gitterman, Mean first passage time for anomalous diffusion. *Phys. Rev.* **62**, 6065–6070 (2000).
38. G. Rangarajan, M. Ding, Anomalous diffusion and the first passage time problem. *Phys. Rev.* **62**, 120–133 (2000).
39. C. Loverdo, O. Bénichou, M. Moreau, R. Voituriez, Enhanced reaction kinetics in biological cells. *Nat. Phys.* **4**, 134–137 (2008).
40. O. Bénichou, C. Loverdo, M. Moreau, R. Voituriez, Intermittent search strategies. *Rev. Mod. Phys.* **83**, 81–129 (2011).
41. A. Godec, R. Metzler, First passage time statistics for two-channel diffusion. *J. Phys. Math. Theor.* **50**, 084001 (2017).
42. D. S. Grebenkov, A unifying approach to first-passage time distributions in diffusing diffusivity and switching diffusion models. *J. Phys. Math. Theor.* **52**, 174001 (2019).
43. P. Illien, T. Adeleke-Larodo, R. Golestanian, Diffusion of an enzyme: The role of fluctuation-induced hydrodynamic coupling. *Europhys. Lett.* **119**, 40002 (2017).
44. T. Adeleke-Larodo, P. Illien, R. Golestanian, Fluctuation-induced hydrodynamic coupling in an asymmetric, anisotropic dumbbell. *European Physical J.* **42**, 39 (2019).
45. J. Agudo-Canalejo, R. Golestanian, Diffusion and steady state distributions of flexible chemotactic enzymes. arXiv:1910.04526 (10 October 2019).
46. R. C. Stewart, R. Van Bruggen, Association and dissociation kinetics for CheY interacting with the P2 domain of CheA. *J. Mol. Biol.* **336**, 287–301 (2004).
47. O. Schon, A. Friedler, M. Bycroft, S. M. Freund, A. R. Fersht, Molecular mechanism of the interaction between MDM2 and p53. *J. Mol. Biol.* **323**, 491–501 (2002).
48. L. Hemsath, R. Dvorsky, D. Fiegen, M. F. Carlier, M. R. Ahmadian, An electrostatic steering mechanism of Cdc42 recognition by Wiskott-Aldrich syndrome proteins. *Mol. Cell* **20**, 313–324 (2005).
49. G. Schreiber, Kinetic studies of protein-protein interactions. *Curr. Opin. Struct. Biol.* **12**, 41–47 (2002).
50. G. Schreiber, G. Haran, H. X. Zhou, Fundamental aspects of protein - protein association kinetics. *Chem. Rev.* **109**, 839–860 (2009).
51. P. Kumar *et al.*, Update of KDBI: Kinetic data of bio-molecular interaction database. *Nucleic Acids Res.* **37**, 636–641 (2009).
52. G. Guntas *et al.*, Engineering an improved light-induced dimer (iLID) for controlling the localization and activity of signaling proteins. *Proc. Nat. Acad. Sci. U.S.A.* **112**, 112–117 (2015).
53. R. D. Skeel, M. Berzins, A method for the spatial discretization of parabolic equations in one space variable. *SIAM J. Sci. Stat. Comput.* **11**, 1–32 (1990).